Express Polymer Letters Vol.17, No.3 (2023) 300–316
Available online at www.expresspolymlett.com
https://doi.org/10.3144/expresspolymlett.2023.22

Research article

Long-chain branched poly(butylene succinate-*co*-terephthalate) copolyesters: Impact of (reactive) synthesis strategies on melt strength properties

Mohamed Yousfi[1,2*], *Cédric Samuel*[1], *Tarek Dadouche*[2], *Rosica Mincheva*[3], *Marie-France Lacrampe*[2]

[1]IMT Nord Europe, Institut Mines-Télécom, Univ. Lille, Centre for Materials and Processes, F-59000 Lille, France
[2]Univ Lyon, CNRS, UMR 5223, Ingénierie des Matériaux Polymères, Université Claude Bernard Lyon 1, INSA Lyon, Université Jean Monnet, F-69621 Villeurbanne, France
[3]Laboratory of Polymeric and Composite Materials (LPCM), University of Mons, Place du Parc, 23, B-7000 Mons, Belgium

Received 21 july 2022; accepted in revised form 3 October 2022

Abstract. Highly biobased poly(butylene succinate-*co*-terephthalate) (PBST) with processing temperatures close to those of commodity polymers (160–180 °C) and long-chain branched architectures (LCB) are synthesized by different strategies. Their rheological properties are investigated, in particular their melt strength properties. A two-step synthesis route is first proposed based on linear LCBs produced by polycondensation followed by reactive extrusion with an epoxy-based multifunctional agent Joncryl® at concentrations up to 2 wt%. A one-step synthesis strategy is also developed using glycerol as a branching agent, introduced at a low concentration (0.5 wt%) directly during the PBST polycondensation process. The molecular weights, LCB structures, and thermal properties are determined by triple detection size exclusion chromatography and differential scanning calorimetry. For PBSTs synthesized in two steps, gelation takes place simultaneously with the branching reactions. However, a concentration of Joncryl® close to 2 wt% is required to improve the melt strength properties, with strain hardening effects under elongation conditions. Interestingly, PBSTs synthesized by *in-situ* addition of glycerol show remarkable melt strength and a high melt stabilization process. Dynamic rheology investigations allow attributing these effects to statistical/homogeneous gel-free LCB architectures obtained during reactive extrusion without any additional post-processing. The effectiveness of approaches to easily improve the melt strength of highly biobased aliphatic-aromatic copolyesters (theoretical biobased content up to 85%) and to eliminate extrusion defects/instabilities in PBSTs is thus demonstrated, allowing the possibility of expanding the industrial application domains of these polymers in packaging and sustainable applications.

Keywords: *biodegradable polymers, rheology, long chain branching, polymer synthesis, molecular engineering*

1. Introduction

Driven by international legislation, end-of-life consideration and treatment of plastic wastes have become major issues for the plastics industry and the academic community. Indeed, the production of plastics is continuously increasing for more than 50 years to reach 368 million tons in 2020 [1]. But, despite many efforts around the world, a large proportion of plastic waste is not recycled, causing significant economic and environmental damage. One possible approach to solving these issues is to replace current petroleum-based thermoplastic polymers with renewable bio-based polymers that are more sustainable. Their ability to compost and/or biodegradability under certain conditions makes them very attractive, in particular for succinic acid (co)polyesters.

*Corresponding author, e-mail: mohamed.yousfi@insa-lyon.fr

However, their processability by conventional technologies of the plastics/textile industry remains rather limited. Indeed, their macromolecular architectures need to be modified by introducing chain extension and/or branching to adapt their rheological properties in the molten state, thus limiting the loss of molecular weight caused by thermal/hydrolytic degradation and widening their processing window by extrusion/injection technologies.

Among succinic acid-based aliphatic (co)polyesters such as poly(butylene succinate) (PBS, Bionolle®, Showa Denko) and poly(butylene succinate-*co*-adipate) (PBSA, BioPBS™, Mitsubishi), aliphatic-aromatic versions such as poly(butylene succinate-*co*-terephthalate) (PBST) represent one of the most promising sustainable polymers due to their renewable/biodegradable nature (high biobased content up to 85%) together with high melting temperatures (150–180 °C) close to those of commodity polyolefins (high-density polyethylene, polypropylene) and polyamides (*e.g.* polyamide 12), high rate of crystallization, excellent shape memory [2] and superior mechanical properties [3, 4].

PBST copolyesters have subsequently received significant attention in the last few years and have been extensively investigated in relation to various research topics including PBST synthesis [5], crystallinity [4], biodegradability [6], gas barrier [7], and mechanical properties [8]. Currently, the main industrial application of PBST is the manufacturing of fibers and yarns used in the textile industry [9].

However, the production of PBST-based items by classical industrial processes such as film blowing, thermoforming, extrusion blow molding, or extrusion foaming processes is hindered by its inadequate rheological behavior. Actually, the rheological and melt strength properties of polymers with linear macromolecular structures are known to induce dramatic processing instabilities, in particular under elongational flows during the above-mentioned processes [10]. On the contrary, polymers with long chain branched (LCB) architectures usually display high viscosities, elasticities, and melt strengths that improve the stability/quality of extruded items and favor recyclability, as the melt rheological properties can be maintained close to those of the original virgin material. Candal *et al*. [11] found that the formation of long-chain branches by reactive extrusion is an efficient way to recycle opaque polyethylene terephthalate (PET) into a new material with enhanced mechanical and rheological performances that are comparable to those of typical virgin PET.

Actually, compared to classical reptation–tube theories of linear polymers, additional relaxation processes are observed for LCB architectures [12] and these architectures particularly require more time to fully relax due to topological constraints at the anchoring points [13–15]. Therefore, under a fast elongational flow, additional stresses are induced that generate strain hardening phenomena of high interest for extrusion processing [15–17]. LCB architectures with high melt strengths could be directly produced during the polymerization process, as depicted in the case of low-density polyethylene produced by free-radical polymerization [18, 19]. The use of specific agents coupled with reactive extrusion processes also represents a widespread method to induce chain extension, crosslink, and to graft reactions leading to LCB architectures [20–23]. It could be noticed that blending and nucleation (with filler or nucleation agent) could also represent alternative approaches to improve the melt strength of thermoplastic polymers [24–28].

In the case of biobased polyesters obtained by polycondensation or ring-opening polymerization and displaying *quasi*-linear architectures, numerous reactive agents are effective in producing LCB architectures with high melt strength for the development of advanced grades [29–33]. The most common way to synthesize LCB co-polyesters is to introduce multifunctional ($f \geq 3$) monomers or oligomers as long chain branching agents, such as multifunctional acids, alcohols, peroxides, isocyanates, and epoxides, in high-temperature polycondensation reaction. Al-Itry *et al*. [34] have used multifunctional epoxy-based agents as chain extenders to adapt the rheological behavior of poly(lactic acid) (PLA) in shear and elongational conditions for the extrusion-blowing process. Li *et al*. [35] have utilized acrylic-based additives to produce LCB-PLA by UV-induced reaction for extrusion foaming processes. Wei and McDonald [31] used peroxide-based agents as crosslinking agents to improve the melt processability of poly(3-hydroxybutyrate). Interestingly, some authors recently considered the case of PBST. Sun *et al*. [36] used epoxy-based agents for the preparation of LCB-PBST. The existence of LCB architectures greatly improved the rheological properties of PBST in shear conditions, but an obvious decrease in ductility is observed. Recently, Lu *et al*. [37] utilized pentaerythritol as a

branching agent for PBST during esterification – polycondensation at 230–250 °C in the presence of a specific catalyst. According to the authors, higher branching efficiencies were attested compared to epoxy-based agents. A slight modification of PBST crystallization parameters is attested for LCB-PBST compared to linear PBST. However, the rheological behavior in elongational conditions of such LCB-PBST has not been documented elsewhere, and, in this context, the efficiency of various reactive agents cannot be clearly concluded.

In the present work, the rheological properties of highly-biobased LCB-PBST in elongational conditions are mainly targeted to fulfill the requirements of industrial elongational processes, in particular, extrusion processing into films. Two different approaches are proposed to synthesize LCB-PBST with melting/processing temperatures close to 160–180 °C (close to those of commodity thermoplastic polymers such as poly(propylene) and Nylon 11).

A classical two-step approach is first proposed based on linear LCBs produced by polycondensation then processes by reactive extrusion with an epoxy-based multifunctional agent Joncryl® at concentrations up to 2 wt%. A one-step approach is also investigated, using glycerol introduced at 0.5 wt% directly during the PBST synthesis by polycondensation. Macromolecular structures and thermal properties of LCB-PBST are evaluated by size-exclusion chromatography (SEC) and differential scanning calorimetry (DSC). Their transient elongational viscosities as a function of the stretching time are then investigated using a rheometer equipped with Sentmanat extensional apparatus. Their linear viscoelastic properties in shear conditions are finally analyzed to depict correlations with macromolecular structures and synthesis strategies.

2. Experimental section

2.1. Materials

Succinic acid (SA, purity 99%, Kosher), 1,4-butanediol (BDO, purity 99%, Kosher), titanium tetra-isopropoxide (TTiPO, purity 98%, Aldrich, USA), and terephthalic acid (TPA, purity 98%, BP Chemicals, UK) were all used as received. Glycerol was purchased from Fisher Scientific, USA. Epoxy-based styrene-acrylic oligomers were kindly supplied by BASF, Germany (Joncryl ADR®-4300F, T_g 56 °C, the epoxy equivalent weight 445 g/mol, molar mass M_w 5500 g/mol, and functionality number (f) is 5) [38]. The general structure of these oligomers designed for chain extension/branching reactions of polyesters, polyamides, and polycarbonates is depicted in Figure 1. The food and drug administration (FDA) compliance was delivered by the European Union for its use in food packaging [39].

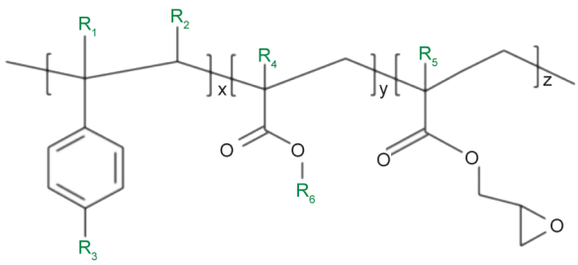

Figure 1. The general structure of epoxy-based styrene-acrylic Joncryl® oligomers (R_1-R_2-R_3-R_4 are H, CH_3, a higher alkyl group, or combinations of them) (R_5 is an alkyl group) (x, y are each between 1 and 20) (z is between 1 and 12) [38].

2.2. One-step synthesis of LCB-PBST by polycondensation

An Autoclave® reactor (Autoclave France, France) specially designed for polycondensation reactions was used. It was equipped with a condenser, a mechanical stirrer, and a vacuum line. The temperature inside the reactor, the pressure, and the torque was monitored during the synthesis. The reactor was fed with TPA and SA powders (molar ratio of TPA to SA equal to 60:40) and a desired amount of BDO was added under stirring. Thereafter, 0.01 mmol of TTiPO used as catalyst was introduced under protective nitrogen flux. The reactor was gradually heated to 210 °C and esterification reactions proceeded at a stirring speed of 80 rpm for 2 hours to produce PBST oligomers. Afterward, glycerol was introduced at a concentration of 0.5 wt% (relative to PBST), and polycondensation reactions were carried out at reduced pressure. For this purpose, the reactor temperature was gradually increased to 250 °C, and the polycondensation reaction was terminated once the stirring torque reached a constant/maximal value. As-prepared PBSTs were dissolved in chloroform and then precipitated in methanol for purification followed by drying in a vacuum oven. The use of glycerol bearing three hydroxyl groups (–OH) is expected to react with PBST carboxyl end groups (–COOH) during polycondensation to form a branching point according to Figure 2.

It should be noted here that long chain branching or crosslinked molecular structures could be obtained according to the glycerol content in the medium [40].

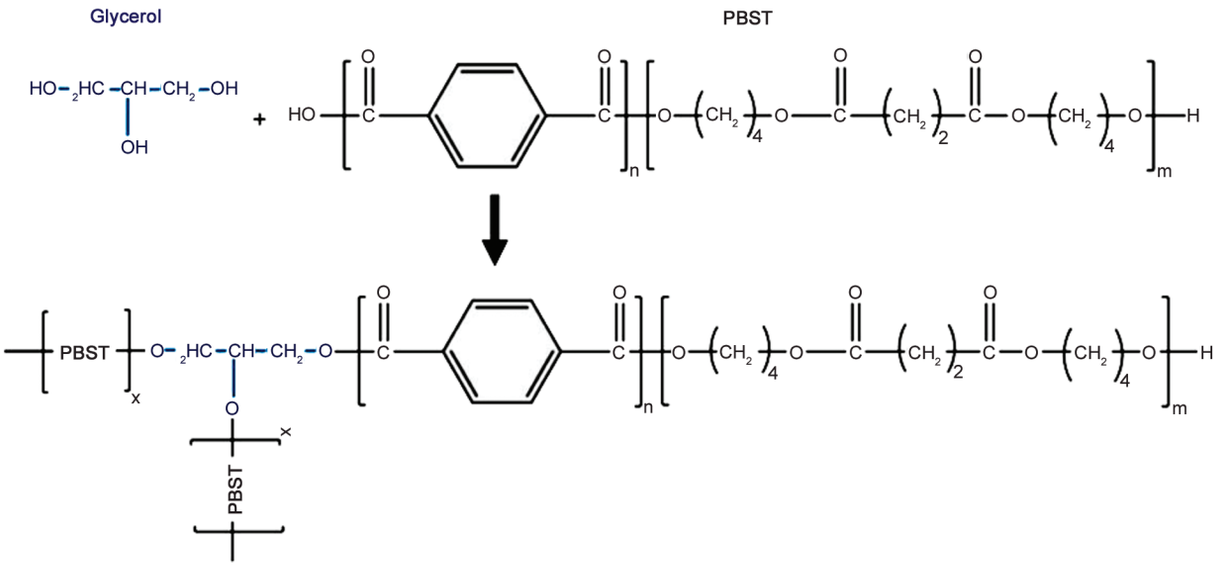

Figure 2. Schematic proposed mechanism for the production of LCB-PBST using glycerol during PBST polycondensation.

In this study, to avoid a possible formation of gels or crosslinked structures, glycerol content was limited to 0.5 wt%. Beyond this concentration, gelification or crosslinking shall occur.

2.3. Two-step synthesis of LCB-PBST by polycondensation – reactive extrusion

The classical two-step synthesis of LCB-PBST involves (i) the production of *quasi*-linear PBST by polycondensation and (ii) reactive extrusion using Joncryl®. The first part is similar to the above procedure, except for the absence of glycerol during polycondensation reactions to yield *quasi*-linear PBST. The second part is performed using a twin-screw μ-extruder (MiniLabII, Thermoscientific, Germany). PBST solids were dried overnight under vacuum at 60 °C and were dry-blended with Joncryl® flakes at concentrations up to 2 wt% just before extrusion. The extrusion temperature is set to 180 °C with a screw speed of 100 rpm for a mixing time of 5 min. The expected mechanisms yielding LCB-PBST by reactive extrusion with Joncryl® are depicted in Figure 3. Finally, all materials were molded into rectangular bars, discs, or cylinders for rheology testing using a Dolouets thermocompression molding machine at 180 °C for 10 min under 80–110 bar. The following Table 1 gathers all PBST materials used in this study with their nomenclature.

2.4. Characterizations

2.4.1. Molecular weight analysis by size-exclusion chromatography (SEC)

Size exclusion chromatography (SEC) was performed on as-prepared materials to determine their molecular weights (M_n, M_w), polydispersity index, and macromolecular architectures. The SEC system is composed of a chromatographic pump (LC-20AD, Shimadzu, Japan), a chromatographic injector (Perkin Elmer Series 200, Germany), one precolumn (PLgel 20 μm Guard 50×7.5 mm, Agilent, Germany) and three columns (PLgel 5 μm Mixed-C, 300×7.5 mm, polystyrene/divinylbenzene stationary phase, Agilent, Germany). The SEC was coupled with a multiangle light scattering detector (WTREOS-01, 3 angles, Wyatt, Germany), a refractometer (RID 10A, Shimadzu, Japan), a UV detector (SPD-20A, Shimadzu, Japan), and a viscosimeter (WVISC-04, Wyatt, Germany). As-prepared PBSTs were dissolved in chloroform at a concentration of 1 mg/ml for 48 h. Solutions were filtrated over polytetrafluoroethylene filters (0.25 μm) to prevent the passage of the gels contained in some LCB-PBSTs into the columns and eluted in the SEC system with chloroform at a flow rate of 1 ml/min. The differential index of refraction dn/dc was measured by a refractometer (Wyatt Optilab T-rex, λ = 658 nm), and a value of 0.08 ml/g was used for data processing.

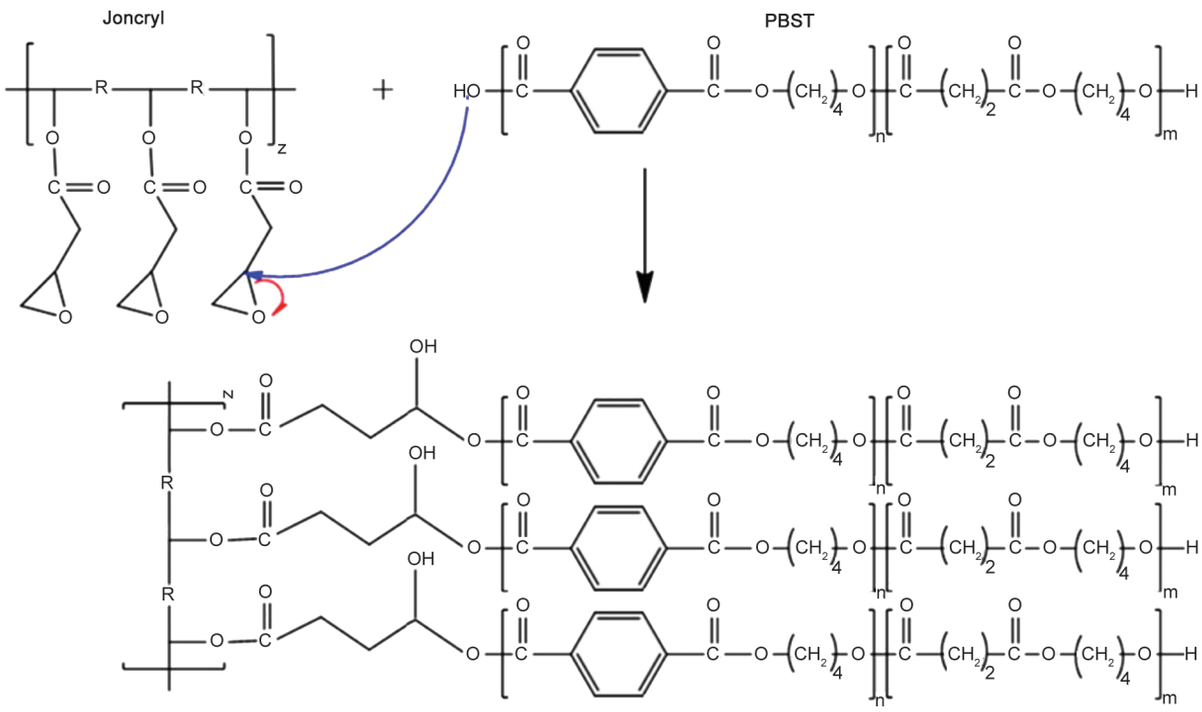

Figure 3. Schematic proposed mechanism for the production of LCB-PBST using epoxy-based styrene-acrylic Joncryl® oligomers.

Table 1. Nomenclature and description of as-prepared PBST.

Nomenclature	Description
L-PBST	Linear PBST synthesized by polycondensation
LCB1-PBST-G	LCB-PBST synthesized by polycondensation using glycerol
LCB2-PBST-J1	LCB-PBST synthesized from L-PBST and reactive extrusion with 1 wt% Joncryl®
LCB2-PBST-J2	LCB-PBST synthesized from L-PBST and reactive extrusion with 2 wt% Joncryl®

2.4.2. Gel determination

It is well-documented in the literature that high contents of a high multifunctional chain extender agent can lead to gelification or even crosslinking. The latter can impact the end-product mechanical performances, like the elongation at break [41]. The linear and LCB-PBST samples were analyzed by the solvent extraction technique [41]. Each sample was dissolved in chloroform without stirring and filtered after 4 days using a 0.2 μm filter. Then, the percentage of gel was determined by weighing residues of insoluble compounds after extraction of the solvent at the end of the drying step in an oven at 50 °C for 48 hours.

2.4.3. Thermal properties by DSC

The thermal properties of the as-prepared materials were determined using a DSC (Mettler Toledo, Switzerland) calibrated with the indium reference (melting point of 156.6 °C). Experiments were carried out under a nitrogen atmosphere with heat – cool – heat cycles at 10 °C/min between –60 to 200 °C. Crystallization temperatures (T_c) were determined during the cooling scan using the exothermic phenomena and melting temperatures (T_m) were determined during the second heating scan using the endothermic phenomena. On the other hand, the glass transition temperature T_g was calculated from the middle point of the step change in heat flow.

2.4.4. Dynamic rheological measurements

Rheological tests in shear conditions were carried out under a nitrogen atmosphere using a stress-controlled dynamic rheometer (Haake MarsIII, Thermo Scientific, Germany). The samples were systematically dried under a vacuum at 60 °C for 24 h before measurement. A parallel-plate geometry (diameter 35 mm) was chosen. Frequency sweeps between 100–0.1 rad/s were performed at 180 °C using a constant strain of 10%. Strain sweeps at a constant angular frequency of 100 rad/s were performed to ensure working into the linear viscoelastic domain for each material.

2.4.5. Elongational rheology measurements

Transient extensional viscosities of as-prepared PBST as a function of the stretching time at various strain rates were evaluated using the previous dynamic rheometer equipped with an SER (Sentmanat Extensional Rheometer, Thermo Scientific, Germany) tool. The working principle is based on two drums attached to the rheometer motor, drums rotating in the opposite direction at the same speed. A pure uniaxial stretching is consequently applied to the test sample. The theoretical details behind the measurement of the transient extensional viscosity are reported in detail by Yousfi *et al*. [28]. Tests were here carried out at 180 °C and, and after rheometer calibration and temperature calibration, the sample was fixed between the two drums. A temperature stabilization period of 120 s was set followed by a pre-stretching step at 300 Pa for 10 s to compensate for sample creep at high temperature. Then, the sample was stretched at a given strain rate (between 0.1–1 s^{-1}). Using the motor torque developed during stretching, the transient extensional viscosity was evaluated. It could be noticed that the SER experimental procedure was optimized on reference low-density polyethylene samples using a video analysis system, in particular, to validate the homogeneity of the applied strain and the true strain rate value.

3. Results and discussions

3.1. Molecular characterization and thermal analysis of as-prepared LCB-PBST

Macromolecular parameters and architectures of as-prepared PBSTs were analyzed by SEC equipped with multiple detection techniques. Therefore, the presence of LCB could be also qualitatively approached to some extent using viscosimetric data. The elution profiles of as-prepared PBST can be found in Figure 4a and 4b with molecular weight distribution profiles and viscosimetric profiles (Figure 4c and 4d). Macromolecular parameters are tabulated in Table 2. The elution profile of L-PBST exhibits a unimodal elution peak, and data processing yields M_n – M_w values close to 20 000–27 000 g/mol for L-PBST. The polydispersity index ($Đ$) of 1.35 is in good accordance with a polycondensation synthesis route [42, 43]. Similar molecular weights (M_w of 28 000 g/mol) and a rather narrow molar mass distribution ($Đ$ of 1.35) were obtained by Ren *et al*. [42] in the case of linear PBSTs produced through traditional polycondensation reaction. Nevertheless, the viscosimetric profile displays a power-law dependence with a power-law index (Mark-Houwink-Sakurada parameter α_{MHS}) close to 0.7–0.73, in agreement with literature data on linear poly(butylene succinate) using the same solvent [44–46]. Garin *et al*. [44] found $[\eta] = 39.9 \cdot 10^{-5} \cdot M_n^{-0.71}$ at 30 °C in chloroform with molecular weights measured by SEC with a triple detection system. These elements confirm the linear architecture of L-PBST as expected with a classical polycondensation synthesis route [47]. Concerning LCB1-PBST-G synthesized by one-step polycondensation using glycerol, the unimodal elution peak is clearly broader and shifted to low elution times. Compared to L-PBST, higher molecular weights and broader molecular weight distributions are obtained with a 1.5-fold increase for M_w and a polydispersity index up to 1.98. The viscosimetric profile also displays a power-law dependence but the power-law index is reduced down to 0.59, indicating the effective presence of LCB in significant amounts [41]. It is useful to mention that gel-free branched PBSTs were obtained when glycerol was used as an LCB agent. Indeed, no insoluble residues were found after solvent removal, and thus no gel was detected.

It can be concluded that a homogenous macromolecular architecture with a statistical distribution of LCB (according to Figure 2) was obtained for LCB1-PBST-G due to the use of glycerol as an LCB branching agent during polycondensation [47]. LCB2-PBST-J1 and LCB2-PBST-J2 synthesized from L-PBST coupled to reactive extrusion with Joncryl® were marked by a complex population of molecular weights and the appearance of a minor population displaying ultra-high molecular weights. From viscosimetric profiles, a significant deviation from the power-law dependence was attested for molecular weights higher than approx. 60 000 g/mol, and a dramatic reduction of the power-law index was observed for molecular weights higher than approx. 100 000 g/mol. In this respect, it could be suspected that (i) the principal population corresponds to initial and unreacted L-PBST with linear architectures, and (ii) the minor population corresponds to the formation of LCB-PBST with a high LCB density [48]. A preferential reactivity between Joncryl® and low-molecular components of L-PBST fits with these observations. Based on molecular weight distribution profiles, the amount of LCB-PBST lies close to 10–20% by weight, depending on Joncryl® concentration. The molecular weights of LCB-PBST seem to lie in the

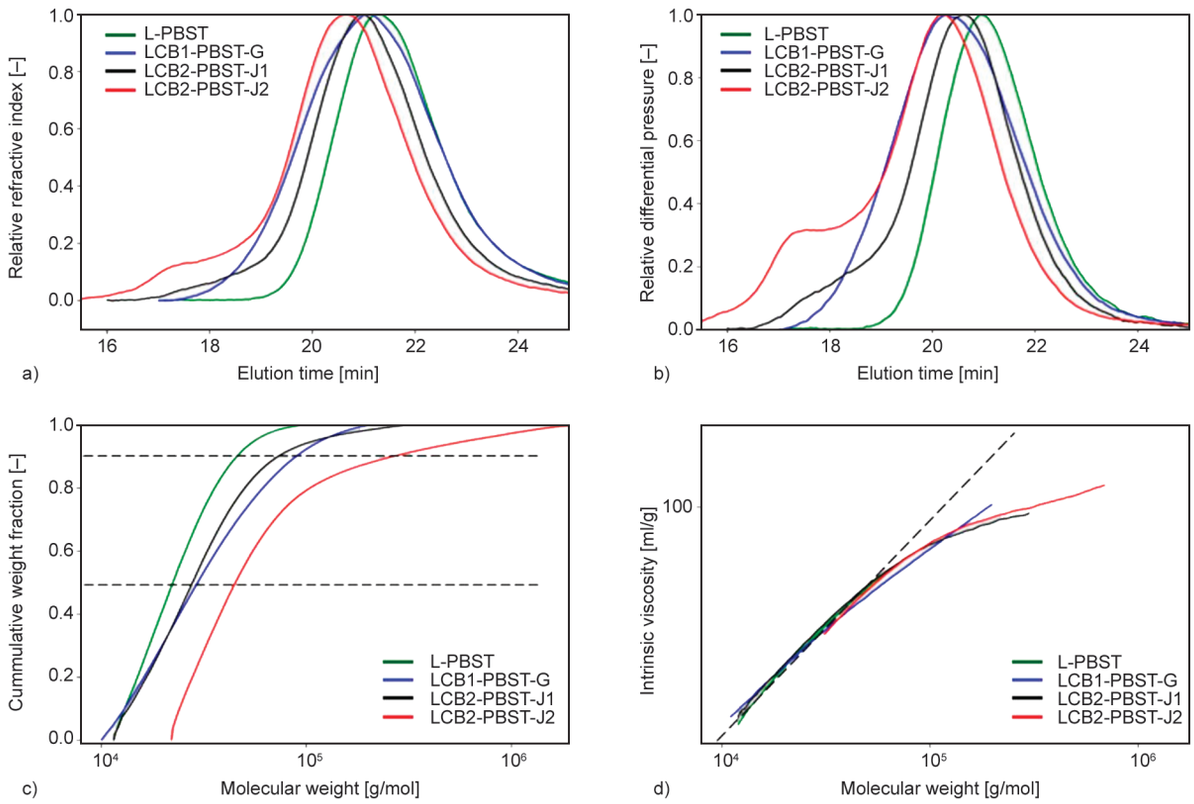

Figure 4. Molecular weight analysis by SEC of as-produced PBST (green L-PBST, blue LCB1-PBST-G, black LCB2-PBST-J1, and red LCB2-PBST-J2). (a, b) Elution profiles (*i.e.*, relative refractive index and relative differential pressure as a function of elution time), (c) molecular weight distribution profiles (*i.e.*, cumulative weight fraction as a function of molecular weight), and (d) viscosimetric profiles (*i.e.*, intrinsic viscosity as a function of molecular weight).

range 60 000–200 000 g/mol in accordance with the reaction scheme displayed in Figure 3 between L-PBST and Joncryl® with an epoxy functionality of 5. Moreover, we note the occurrence of partial gelification of PBST for high Joncryl® concentrations due to side reactions. The gel content was 35±1.2 wt% for LCB2-PBST-J2 and 15±0.9 wt% for LCB2-PBST-J1, as proven by solvent extraction. It has been reported in several literatures reports that the addition of Joncryl beyond 0.6 wt% could change the structure of LCB-polymers toward the sol–gel transition point [48]. Thus, a high Joncryl content can lead to excessive branching and even crosslinking, which was responsible for the formation of gel [47]. The two-step approach by reactive extrusion with Joncryl® clearly yields heterogenous macromolecular architectures comprising initial linear L-PBST and LCB-PBST with a high LCB density. In conclusion, LCB-PBST was efficiently produced by the two proposed synthesis approaches, but different macromolecular architectures were clearly achieved for LCB1-PBST-G and LCB2-PBST-J1/2.

As mentioned earlier, glycerol has three reactive hydroxyl groups (two primary hydroxyl groups and one secondary hydroxyl group). Thus, glycerol could be considered as a tri-functional additive in polycondensation reactions leading to branching points on the PBST backbone (in accordance with higher molecular

Table 2. Macromolecular parameters of as-produced PBST (number average molecular weight M_n, weight average molecular weight M_w, polydispersity index $Đ = M_w/M_n$, and Mark-Houwink-Sakurada parameter α_{MHS}, n.d. not determined).

Sample	M_n [g/mol]	M_w [g/mol]	$Đ$ [–]	α_{MHS} [–]	Gel content [wt%]
L-PBST	20 000	27 000	1.35	0.70–0.73	0
LCB1-PBST-G	22 000	43 000	1.98	0.59	0
LCB2-PBST-J1	23 000	32 000	1.38	n.d.	15.0±0.9
LCB2-PBST-J2	41 000	145 000	3.50	n.d.	35.0±1.2

weights and architectures detected by SEC). Glycerol seems to have a comparable efficiency with tris(hydroxymethyl)ethane for polyester branching. It can be noticed that Nifant'ev *et al*. [48] found similar results when using glycerol as a long chain branching agent (LCB) of poly(butylene adipate terephthalate) (PBAT). However, the M_w of PBAT copolymers obtained in the presence of trimethyl 1,3,5-benzenetricarboxylate (tri-ester-based LCB) was lower in comparison with the M_w of the PBAT synthesized with the use of glycerol. According to the authors, this was due to the lower reactivity of aromatic esters in polycondensation compared to aliphatic $–CH_2OH$ functional groups present in glycerol.

Typical DSC thermograms are displayed in Figure 5 for L-PBST and LCB1-PBST-G that clearly attest for semi-crystalline thermoplastic materials. Thermal parameters are tabulated in Table 3. Concerning L-PBST, a glass transition temperature of –16.5 °C was recorded with a crystallization temperature of 130.9 °C. Two distinct shoulder melting peaks located at 156.2 and 165.5 °C were observed which could be ascribed to the recrystallization and remelting mechanism [43, 49]. Indeed, Jie *et al*. [50] provided direct evidence to support this mechanism through the study by modulated differential scanning calorimetry. In this study, the obtained DSC values were in accordance with bibliographic data concerning various linear PBSTs [51–53]. It can be interestingly noticed that the thermal properties of L-PBST can be tuned and get closer to those of commodity polyolefins according to the molar ratio (X_{mol}) of TPA to SA during synthesis (*i.e.* the content of butylene terephtalate (BT) comonomer in the composition). When X_{mol} is equal to 35:65, L-PBST displays thermal parameters (glass transition temperature T_g, melting temperature T_m, crystallization temperature T_c) close to those of low-density poly(ethylene). And *vice versa*, when X_{mol} is around 66:34, L-PBST possesses thermal characteristics close to those of isotactic poly(propylene) as seen in Table 3 [53, 54].

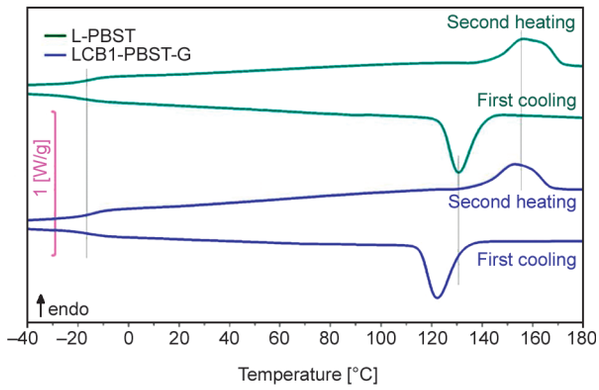

Figure 5. DSC traces (first cooling scan and second heating scan at 10 °C/min) were obtained for L-PBST and LCB1-PBST-G.

The crystallinity of L-PBST still remains challenging to address because the melting enthalpy of fully-crystalline PBST is largely unknown, but crystallization/melting enthalpy seems to be close to various semi-crystalline aliphatic(-aromatic) polyesters such as poly(butylene succinate) and poly(butylenes terephthalate) [55–57].

From DSC data, it was found that the crystallization temperature (T_c) increased first and then decreased with the increase in Joncryl content. The crystallization was first favored probably because of enhanced mobility of chains, but excessive branching (2 wt% of joncryl) led to less regularity of macromolecular chains and consequently retarded crystallization. Similar trends were observed by Lu *et al*. [37] in the case of PBST modified by pentaerythritol (PER) used as a branching agent. In the case of LCB1-PBST-G, the decrease in the crystallization temperature (T_c)

Table 3. Thermal properties of as-produced PBST (glass transition temperature T_g, melting temperature T_m, crystallization temperature T_c and their associated enthalpies).

Sample	T_g[a] [°C]	T_m[a] [°C]		ΔH_m[a] [J/g]	T_c[b] [°C]	ΔH_c[a] [J/g]
		$T_{m,1}$[a]	$T_{m,2}$[a]			
L-PBST	–16.5	156.2	165.5	27.8	130.9	27.4
LCB1-PBST-G	–16.1	152.7	160.1	26.5	122.4	25.9
LCB2-PBST-J1	–16.0	158.8	167.4	25.0	133.9	24.2
LCB2-PBST-J2	–14.0	157.9	166.1	24.2	127.5	23.7
iPP[c]	–10.0	–	165.6	117.0	122.7	111.0

[a]Evaluated at the second heating scan
[b]Evaluated at the first cooling scan
[c]Data from Purohit *et al*. [60].

could be explained by the increase in intermolecular entanglement induced by branching with glycerol. Such increased molecular entanglement reduces segmental mobility leading to the lower T_c. On the other hand, similar glass transition temperatures close to –16 °C are reported for L-PBST, LCB1-PBST-G, and LCB2-PBST-J1, except for a slight increase to –14 °C for LCB2-PBST-J2 that could be linked to segmental mobility hindrance for elevated LCB density [58]. The main phenomenon lies in a significant reduction of the melting/crystallization temperatures for LCB1-PBST-G compared to L-PBST. Reduced melting/crystallization temperatures suggest significant modification of the crystal nucleation/growth mechanisms and the production of defective crystals due to LCB [58, 59].

It can be interestingly noticed that this phenomenon confirms the statistical/homogenous architecture for LCB1-PBST-G. In conclusion, semi-crystalline LCB-PBSTs with glass transition temperatures below room temperature were obtained. Thermal properties were close to those of commodity polyolefins, in particular, isotactic poly(propylene) for these highly-biobased LCB-PBSTs, and processing temperatures could be set to 160–180 °C [3]. Moderate modifications of thermal properties were attested for LCB-PBSTs, but correlations to LCB architectures were detected, *i.e.*, statistical/homogenous architectures for LCB1-PBST-G and production of highly-branched architectures for LCB2-PBST-J2.

3.2. Melt-state rheological stability of as-prepared LCB-PBST

The macromolecular structure of polyesters could be evolved at high temperatures, in particular at relevant processing temperatures in the melt state. A reduction of their melt viscosity at elevated residence times is often observed due to macromolecular degradation. Several degradation reactions could be encountered for polyesters, such as (i) hydrolytic/mechanical degradation with random chain scission along polyester chains (ii) and degradation by hydrogen transfer with a localized chain scission close to end-chains, and production of small molecules [61–65]. The use of Joncryl® is known to improve the viscosity of polyesters (according to Figure 3) and compensate for viscosity drops due to chain degradation/chain branching recombination reactions [34]. The complex viscosity and the magnitude of degradation reactions were subsequently evaluated by dynamic rheology for as-prepared LCB-PBST. Time sweep tests at 180 °C and 10 rad/s in the linear regime were carried out, and the results are presented in Figure 6.

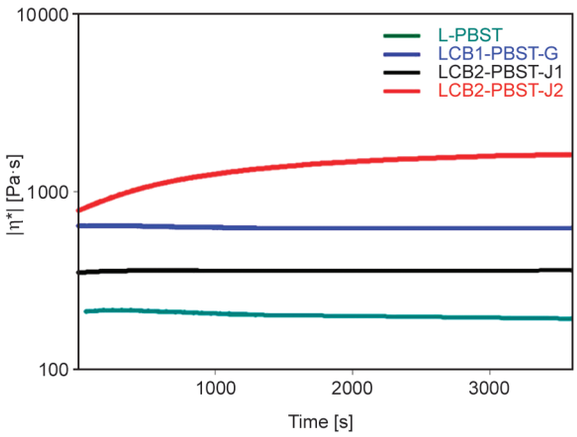

Figure 6. Evolution of the complex viscosity versus time at 180 °C for as-prepared PBST.

The initial complex viscosity of L-PBST was close to 210 Pa·s, and a slight degradation of L-PBST was observed with a continuous viscosity drop up to 190 Pa·s in approx. 1 h. A higher complex viscosity was evidenced for LCB1-PBST-G with an initial complex viscosity of 660 Pa·s, and LCB1-PBST-G also slightly degraded with a viscosity drop to 620 Pa·s in 1 h. The degradation of L-PBST and LCB-PBST-G in the melt state was consequently found quite slow. This slight degradation behavior is probably linked to (i) the low residual water content after appropriate drying and (ii) the low processing temperature of these polyesters. Concerning LCB2-PBST-J1 and LCB2-PBST-J2, their initial complex viscosities were evaluated to 360 and 780 Pa·s as classical effects encountered with the use of Joncryl®. It can be noticed that the complex viscosity of LCB2-PBST-J1 was highly stable over time which corresponds to a perfect balance between chain degradation/recombination reactions. For LCB2-PBST-J2, a high increase in viscosity was observed as a function of time, and a stable value was achieved after a residence time of 1 h at 180 °C. Based on these rheological results, *quasi*-stable rheological parameters in shear conditions were concluded for L-PBST, LCB1-PBST-G, and LCB2-PBST-J1. Higher viscosities were also detected for LCB1-PBST-G and LCB2-PBST-J1 in accordance with previous macromolecular analyses (higher M_w, higher polydispersity index, and presence of LCB in significant amounts). LCB2-PBST-J2 displayed an unstable rheological behavior due to intensive chain recombination reactions.

3.3. Shear rheological properties of as-prepared LCB-PBST

L-PBST displayed a constant complex viscosity (η^*) over the entire frequency range with a Newtonian viscosity (or zero-shear viscosity at low frequency) close to 200 Pa·s. in accordance with relatively low molecular weights for L-PBST (Figure 7). A significant increase in Newtonian viscosity was observed for LCB1-PBST-G, and the evolution of the storage modulus (G') (at low frequencies displayed a classical trend with a slope of approx. 2. The rheological behaviors of the two-step chain-extended LCB2-PBST-J1/2 were quite different from PBST produced by the one-step route with glycerol (LCB1-PBST-G). LCB2-PBST-J1 only displayed a moderate increase in Newtonian viscosity, but the evolution of the storage modulus G' at low frequencies displayed a lower slope. Noting that LCB2-PBST-J1 contains 15% of gels but still had a Newtonian viscosity plateau at low frequencies, which suggests that these gels may have crosslink points of low densities and are partially miscible with the linear and branched chains [66]. For LCB2-PBST-J2, the complex viscosity strongly increased at low frequencies. The storage modulus G' also reached a plateau at a low frequency for LCB2-PBST-J2, which is related to a long-time-relaxation mechanism due to the formation of long-chain branches (LCB) during reactive extrusion with Joncryl [27, 67] and to the presence of the high amount of gels (35 wt%) in the structure.

It is useful to mention that a pronounced shear thinning behavior was found at high frequencies for the LCB-PBST samples compared to L-PBST [68]. The pseudoplasticity indices were 0.86, 0.66, and 0.60 for LCB2-PBST-J1, LCB1-PBST-G, and LCB2-PBST-J2, respectively. According to the literature [41], this non-Newtonian behavior is the result of long-chain branching (*i.e.*, the increased molecular entanglement of the branched structure) and a broadening of the molecular weight distribution (demonstrated by SEC measurements). Such behavior has been correlated with better melt processability by film blowing and extrusion foaming by gas injection (the increased elasticity would hinder the cell coalescence and cell wall rupture) [48, 67, 68].

The relaxation spectra $H(\lambda)$ at 180 °C of as-produced PBST were calculated from G' data using the standard nonlinear regularization method proposed by Honerkamp and Weese [69]. Results are shown in Figure 7c. The relaxation peak of L-PBST cannot be identified in the frequency range studied. The relaxation time of L-PBST was consequently very fast and probably lower than 0.01 s. However, two relaxation peaks were clearly attested for LCB-PBST-G, with a first peak close to 0.15 s and a second close to 1 s. This phenomenon can be interpreted by the presence of two modes of relaxation, with a first relaxation mode corresponding to the relaxation of LCB and a second relaxation mode corresponding to the PBST backbone with restricted mobility [23, 67]. These phenomena clearly attested to the presence of LCB in low amounts along the PBST backbone. LCB2-PBST-J1 displayed a unique relaxation peak close to 0.9 s, and the relaxation peak of LCB2-PBST-J2 cannot be identified in the frequency range studied. The presence of complex LCB architectures without relaxation modes for the PBST backbone was thus suspected for LCB2-PBST-J1/2 [28, 70].

Figure 8 shows the results of the reduced Van–Gurp–Palmen diagram (rVGP) at 180 °C of as-produced PBST. An rVGP diagram is made up with loss angle δ against the reduced modulus G_{red} (complex modulus G^* divided by the plateau modulus G_N^0, evaluated at high frequencies when phase angle δ tends to 0). According to Trinkle *et al*. [71], the shape of the rVGP diagram is unaffected by the molecular weight, but the polydispersity index/LCB architectures have specific signatures [28, 70]. The rVGP diagram is consequently a clear way to assess chain topologies. It is clear that L-PBST displayed a viscous behavior at low G_{red}. The phase angle sharply decreased for G_{red} values above approx. 0.1 as a typical signature of linear thermoplastic polymers with a narrow polydispersity index [71]. The rheological responses of L-PBST (frequency sweeps, relaxation spectra, and rVGP diagram) were consistent with previous conclusions by SEC (moderate molecular weight, narrow polydispersity index, and linear architectures). For LCB1-PBST-G, the phase angle started to decrease for G_{red} values above 0.01 and the phase angle drop was slightly broader than that of L-PBST. This rVPG behavior can be mainly ascribed to the high polydispersity of LCB1-PBST-G. A slight inflection point was noticed for phase angle close to 50° and G_{red} close to 1. No clear similitude with model chain topology was attested but this critical point of low intensity could correspond to comb-like architectures with LCB and PBST backbones displaying similar molecular weights [71]. The LCB density along the PBST backbone is probably quite low. The

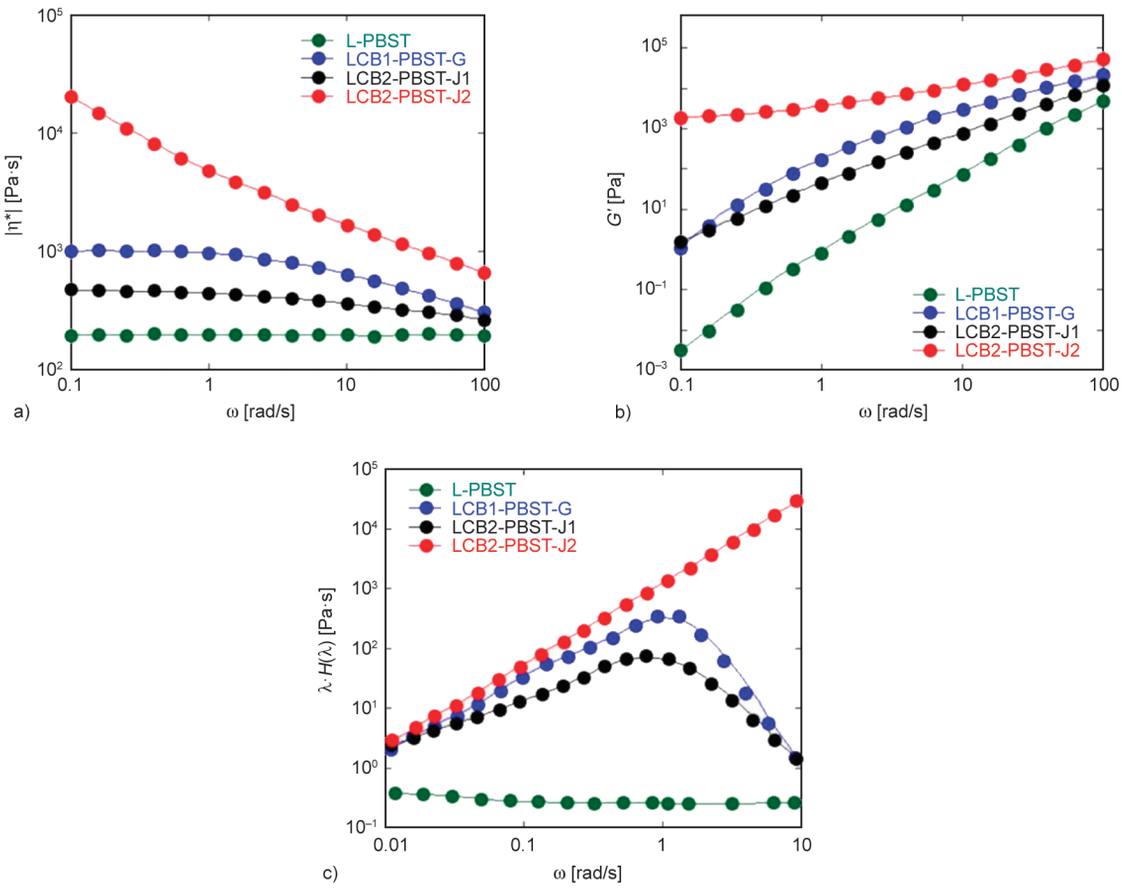

Figure 7. Complex viscosity (a) and storage modulus (b) at 180 °C of as-prepared PBST. Weighted relaxation time spectrum at 180 °C of as-prepared PBST (c).

rheological responses of LCB1-PBST-G consequently fitted with previous conclusions by SEC (high/broad molecular weight, presence of LCB in low amount, statistical/homogeneous distribution of LCB along the PBST backbone, similar molecular weights for LCB/backbone). It could be also noticed that the rVGP diagram was quite similar to that of strain-hardening metallocene polyethylene [72], indicating that the rheological response in elongational conditions of LCB1-PBST-G could be of good interest.

Concerning LCB2-PBST-J1 and LCB2-PBST-J2, the rVGP diagrams were quite different from those of LCB1-PBST-G. LCB1-PBST-J1 displayed a mixed behavior between L-PBST and LCB1-PBST-G. The presence of LCB was suspected in a low amount, along with unreacted L-PBST. No inflection was noticed for LCB1-PBST-J1. LCB2-PBST-J2 displayed phase angles lower than 40–50° for any G_{red}. The phase angle also decreased in the low G_{red} region with maximum observed for G_{red} values close to 0.2. This behavior was in agreement with an elastic

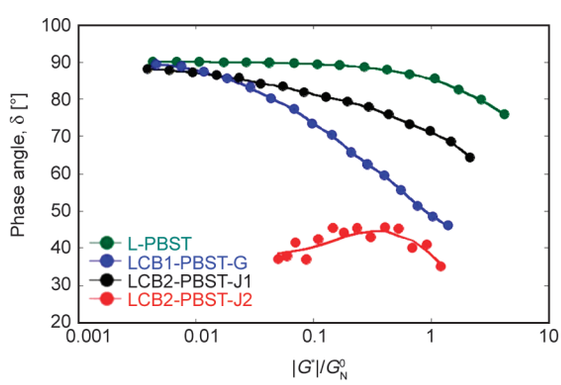

Figure 8. Reduced Van–Gurp–Palmen diagram at 180 °C of as-prepared PBST.

behavior at low frequencies and, according to Trinkle *et al*. [71], this rVGP diagram probably fitted with star-like LCB architectures with high entanglement density. The rheological responses of LCB2-PBST-J1 and LCB2-PBST-J2 could consequently agree with previous conclusions by SEC (residual L-PBST fraction, the appearance of LCB-PBST structures with a high LCB density, partial gelification/cross-linking).

3.4. Elongational rheological behavior of as-prepared LCB-PBST

LCB architectures are known to improve the rheological behavior of polymer melts in elongational flow conditions marked by higher melt strengths (or transient elongational viscosity) and the appearance of a strain hardening phenomenon. Processing defects and instabilities are drastically reduced for polymers displaying LCB architectures, in particular during extrusion processing (extrusion casting/calendaring, extrusion blowing, co-extrusion, extrusion blow molding, *etc*.) [11]. In this context, the rheological behavior of as-prepared LCB-PBST in elongational conditions was investigated to identify their processability potential by extrusion.

LCB-PBST were uniaxially-stretched in the molten state at 180 °C at different strain rates (between 0.1 and 1 s^{-1}) in order to assess their transient elongational viscosity (η_E) as a function of stretching time (Figure 9). The transient elongational viscosity of L-PBST could not be evaluated due to a poor melt strength inducing an intensive creep before stretching in the melt state. Such behavior is typically observed with thermoplastic polymers displaying moderate molecular weights and linear architectures [11, 26]. These materials do not exhibit any strain hardening phenomena in elongational flow conditions [11, 26], and as-prepared L-PBST is consequently of poor interest for further processing by extrusion.

Concerning LCB2-PBST-J1, a significant melt strength was obtained with a transient elongational viscosity close to 2000–3000 Pa·s at 0.1 s^{-1}. However, no strain hardening phenomenon was detected at any strain rate. The amount of LCB was, therefore, not sufficient to induce strong modifications of the rheological behavior in elongational flow conditions. However, LCB2-PBST-J2 displayed a high melt strength close to 10 000 Pa·s at a low stretching time for any strain rate with an intense strain hardening. Such behavior indicates that LCB2-PBST-J2 exhibits relaxation times higher than approx. 1 s [73], in accordance with previous rheological behavior in shear conditions. As a consequence, the two-step synthesis route requires Joncryl® concentrations close to 2 wt% to produce LCB-PBST with a suitable rheological behavior for further extrusion processing due to adequate LCB architectures (amount/topology). LCB1-PBST-G interestingly displayed a high melt strength close to 8000–10 000 Pa·s at a low stretching time. A strain hardening phenomenon

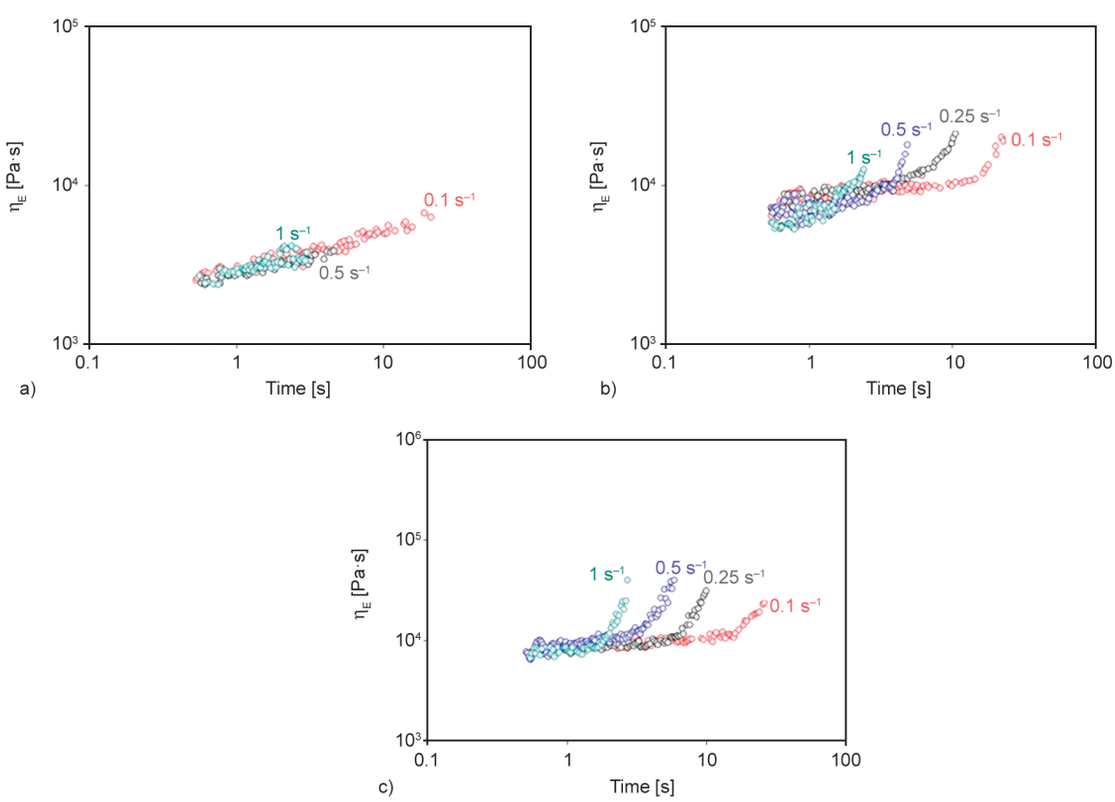

Figure 9. Transient elongational viscosity at 180 °C as a function of stretching time and strain rate for LCB2-PBST-J1 (a), LCB1-PBST-G (b), and LCB2-PBST-J2 (c).

was also observed with a slightly lower intensity than that of LCB2-PBST-J2. These observations were in accordance with the rheological behavior in shear conditions of LCB1-PBST-G, in particular, the detection of relaxation times higher than 1 s. Nevertheless, the pronounced elongational features of LCB1-PBST-G compared to L-PBST could eventually significantly improve stretching ability, stability in thickness, and resistance to melting breakup for processing applications (*e.g.*, extrusion film blowing) where the strain hardening plays an important role [74, 75].

4. Conclusions

Highly-biobased poly(butylene succinate-*co*-terephthalate) (PBST) (potential biobased content close to 85%) with processing temperatures close to those of commodity polymers (160–180 °C) and long-chain branched (LCB) architectures were successfully synthesized by various strategies. The two-step synthesis route starting from linear PBST produced by polycondensation followed by reactive extrusion required a concentration of Joncryl® close to 2 wt% to improve melt strength properties of PBST and induce strain hardening phenomenon effects in elongational conditions.

In this context, it could be concluded that LCB-PBST with an appropriate rheological behavior for further extrusion processing could be directly obtained without any additional post-treatments by reactive extrusion by the one-step synthesis route using glycerol in low concentration (up to 0.5 wt%) during PBST polycondensation. The use of Joncryl® with intense rheological instabilities (*e.g.*, the melt reaction that often continues over time with the unpredictable process and end-product characteristics) in addition to gel formation (problematic recycling capabilities) could be particularly avoided with this approach. The peculiar LCB architecture (high/broad molecular weight, statistical/homogeneous distribution of LCB along the PBST backbone without the formation of gels) probably represents a key element to reaching such rheological behavior due to a significant modification of relaxation dynamics of the PBST backbone.

This work provided an effective approach based on the one-step synthesis method to improve the melt strength of highly-biobased aliphatic-aromatic copolyesters and eliminate extrusion defects/instabilities of PBST using glycerol as a promising long-chain branching agent. This may expand the industrial implementation of these polymers with modern continuous technology production into high-value packaging applications.

Acknowledgements

The authors gratefully acknowledge Ms. Agnes Crepet from the University Claude Bernard Lyon 1 and Mr. Ahmed Belhadj from INSA Lyon for their experimental support and recommendations regarding the SEC-MALS and gel determination measurements. The authors acknowledge the European Community (FEDER funds) and the International Campus on Safety and Intermodality in Transportation (CISIT, France) as well as the Hauts-de-France Region (France) for the financial contribution of the dynamic rheometer and extrusion machines.

References

[1] Marinova D., Bogueva D.: Reducing food waste and packaging. in 'Food in a planetary emergency' (eds.: Marinova D., Bogueva D.) Springer, Singapore, 57–72 (2022). https://doi.org/10.1007/978-981-16-7707-6_4

[2] Shi Y., Zheng C., Zhu G., Ren Y., Liu L-Z., Zhang W., Han L.: A heat initiated 3D shape recovery and biodegradable thermoplastic tolerating a strain of 5. Reactive and Functional Polymers, **154**, 104680 (2020). https://doi.org/10.1016/j.reactfunctpolym.2020.104680

[3] Jacquel N., Saint-Loup R., Pascault J-P., Rousseau A., Fenouillot F.: Bio-based alternatives in the synthesis of aliphatic–aromatic polyesters dedicated to biodegradable film applications. Polymer, **59**, 234–242 (2015). https://doi.org/10.1016/j.polymer.2014.12.021

[4] Li F., Luo S., Ma C., Yu J., Cao A.: The crystallization and morphology of biodegradable poly(butylene succinate-*co*-terephthalate) copolyesters with high content of BT units. Journal of Applied Polymer Science, **118**, 623–630 (2010). https://doi.org/10.1002/app.32381

[5] Tsai P-H., Wang C-H., Kan L-S., Chen C. W.: Studies on the optimal conditions for synthesizing poly(butylene succinate-*co*-terephthalate) copolyesters with targeted properties. Asia-Pacific Journal of Chemical Engineering, **7**, S88-S94 (2012). https://doi.org/10.1002/apj.645

[6] Honda N., Taniguchi I., Miyamoto M., Kimura Y.: Reaction mechanism of enzymatic degradation of poly (butylene succinate-*co*-terephthalate) (PBST) with a lipase originated from *Pseudomonas cepacia*. Macromolecular Bioscience, **3**, 189–197 (2003). https://doi.org/10.1002/mabi.200390023

[7] Qin P., Wu L., Li B., Li N., Pan X., Dai J.: Superior gas barrier properties of biodegradable PBST *vs*. PBAT copolyesters: A comparative study. Polymers, **13**, 3449 (2021). https://doi.org/10.3390/polym13193449

[8] Li F., Luo S., Zhang J., Yu J.: Temperature dependences of solid structure and properties of biodegradable poly(butylene succinate-*co*-terephthalate) (PBST) copolyester. Journal of Thermal Analysis and Calorimetry, **113**, 915–921 (2013). https://doi.org/10.1007/s10973-012-2772-x

[9] Zhang J., Wang X., Li F., Yu J.: Mechanical properties and crystal structure transition of biodegradable poly (butylene succinate-*co*-terephthalate) (PBST) fibers. Fibers and Polymers, **13**, 1233–1238 (2012). https://doi.org/10.1007/s12221-012-1233-2

[10] Xu M., Lu J., Zhao J., Wei L., Liu T., Zhao L., Park C. B.: Rheological and foaming behaviors of long-chain branched polyamide 6 with controlled branch length. Polymer, **224**, 123730 (2021). https://doi.org/10.1016/j.polymer.2021.123730

[11] Candal M. V., Safari M., Fernández M., Otaegi I., Múgica A., Zubitur M., Gerrica-Echevarria G., Sebastián V., Irusta S., Loaeza D., Maspoch M. L., Santana O. O., Müller A. J.: Structure and properties of reactively extruded opaque post-consumer recycled PET. Polymers, **13**, 3531 (2021). https://doi.org/10.3390/polym13203531

[12] Seo Y. P., Seo Y.: Effect of molecular structure change on the melt rheological properties of a polyamide (nylon 6). ACS omega, **3**, 16549–16555 (2018). https://doi.org/10.1021/acsomega.8b02355

[13] Larson R. G., Zhou Q., Shanbhag S., Park S. J.: Advances in modeling of polymer melt rheology. AIChE Journal, **53**, 542–548 (2007). https://doi.org/10.1002/aic.11064

[14] Liu J., Yu W., Zhou C.: Polymer chain topological map as determined by linear viscoelasticity. Journal of Rheology, **55**, 545–570 (2011). https://doi.org/10.1122/1.3569136

[15] Narimissa E., Wagner M. H.: Review on tube model based constitutive equations for polydisperse linear and long-chain branched polymer melts. Journal of Rheology, **63**, 361–375 (2019). https://doi.org/10.1122/1.5064642

[16] Al-Itry R., Lamnawar K., Maazouz A.: Biopolymer blends based on poly(lactic acid): Shear and elongation rheology/structure/blowing process relationships. Polymers, **7**, 939–962 (2015). https://doi.org/10.3390/polym7050939

[17] Sugimoto M., Tanaka T., Masubuchi Y., Takimoto J-I., Koyama K.: Effect of chain structure on the melt rheology of modified polypropylene. Journal of Applied Polymer Science, **73**, 1493–1500 (1999). https://doi.org/10.1002/(SICI)1097-4628(19990822)73:8<1493::AID-APP18>3.0.CO;2-2

[18] Yan D., Wang W-J., Zhu S.: Effect of long chain branching on rheological properties of metallocene polyethylene. Polymer, **40**, 1737–1744 (1999). https://doi.org/10.1016/S0032-3861(98)00318-8

[19] Romanini D., Savadori A., Gianotti G.: Long chain branching in low density polyethylene: 2. Rheological behaviour of the polymers. Polymer, **21**, 1092–1101 (1980). https://doi.org/10.1016/0032-3861(80)90045-2

[20] Forsythe J. S., Cheah K., Nisbet D. R., Gupta R. K., Lau A., Donovan A. R., O'Shea M. S., Moad G.: Rheological properties of high melt strength poly(ethylene terephthalate) formed by reactive extrusion. Journal of Applied Polymer Science, **100**, 3646–3652 (2006). https://doi.org/10.1002/app.23166

[21] Cao K., Li Y., Lu Z-Q., Wu S-L., Chen Z-H., Yao Z., Huang Z-M.: Preparation and characterization of high melt strength polypropylene with long chain branched structure by the reactive extrusion process. Journal of Applied Polymer Science, **121**, 3384–3392 (2011). https://doi.org/10.1002/app.34007

[22] Stanic S., Gottlieb G., Koch T., Göpperl L., Schmid K., Knaus S., Archodoulaki V-M.: Influence of different types of peroxides on the long-chain branching of PP *via* reactive extrusion. Polymers, **12**, 886 (2020). https://doi.org/10.3390/polym12040886

[23] Corre Y-M., Duchet J., Reignier J., Maazouz A.: Melt strengthening of poly(lactic acid) through reactive extrusion with epoxy-functionalized chains. Rheologica Acta, **50**, 613–629 (2011). https://doi.org/10.1007/s00397-011-0538-1

[24] Wang L., Jing X., Cheng H., Hu X., Yang L., Huang Y.: Blends of linear and long-chain branched poly(L-lactide)s with high melt strength and fast crystallization rate. Industrial and Engineering Chemistry Research, **51**, 10088–10099 (2012). https://doi.org/10.1021/ie300526u

[25] Zhang H., Bai H., Liu Z., Zhang Q., Fu Q.: Toward high-performance poly(L-lactide) fibers *via* tailoring crystallization with the aid of fibrillar nucleating agent. ACS Sustainable Chemistry and Engineering, **4**, 3939–3947 (2016). https://doi.org/10.1021/acssuschemeng.6b00784

[26] Dadouche T., Yousfi M., Samuel C., Lacrampe M-F., Soulestin J.: (Nano)fibrillar morphology development in biobased poly(butylene succinate-*co*-adipate)/poly (amide-11) blown films. Polymer Engineering and Science, **61**, 1324–1337 (2021). https://doi.org/10.1002/pen.25645

[27] Yousfi M., Dadouche T., Chomat D., Samuel C., Soulestin J., Lacrampe M-F., Krawczak P.: Development of nanofibrillar morphologies in poly(L-lactide)/poly(amide) blends: Role of the matrix elasticity and identification of the critical shear rate for the nodular/fibrillar transition. RSC Advances, **8**, 22023–22041 (2018). https://doi.org/10.1039/C8RA03339K

[28] Yousfi M., Soulestin J., Marcille S., Lacrampe M-F.: *In-situ* nano-fibrillation of poly(butylene succinate-*co*-adipate) in isosorbide-based polycarbonate matrix. Relationship between rheological parameters and induced morphological and mechanical properties. Polymer, **217**, 123445 (2021). https://doi.org/10.1016/j.polymer.2021.123445

[29] Zhang Z., Wan D., Xing H., Zhang Z., Tan H., Wang L., Zheng J., An Y., Tang T.: A new grafting monomer for synthesizing long chain branched polypropylene through melt radical reaction. Polymer, **53**, 121–129 (2012). https://doi.org/10.1016/j.polymer.2011.11.033

[30] Wang L., Jing X., Cheng H., Hu X., Yang L., Huang Y.: Rheology and crystallization of long-chain branched poly(L-lactide)s with controlled branch length. Industrial and Engineering Chemistry Research, **51**, 10731–10741 (2012). https://doi.org/10.1021/ie300524j

[31] Wei L., McDonald A. G.: Peroxide induced cross-linking by reactive melt processing of two biopolyesters: Poly(3-hydroxybutyrate) and poly(L-lactic acid) to improve their melting processability. Journal of Applied Polymer Science, **132**, 41724 (2015). https://doi.org/10.1002/app.41724

[32] Przybysz-Romatowska M., Haponiuk J., Formela K.: Reactive extrusion of biodegradable aliphatic polyesters in the presence of free-radical-initiators: A review. Polymer Degradation and Stability, **182**, 109383 (2020). https://doi.org/10.1016/j.polymdegradstab.2020.109383

[33] Reichert C. L., Bugnicourt E., Coltelli M-B., Cinelli P., Lazzeri A., Canesi I., Braca F., Martínez B. M., Alonso R., Agostinis L., Verstichel S., Six L., de Mets S., Gómez E. C., Ißbrücker C., Geerinck R., Nettleton D. F., Campos I., Sauter E., Pieczyk P., Schmid M.: Bio-based packaging: Materials, modifications, industrial applications and sustainability. Polymers, **12**, 1558 (2020). https://doi.org/10.3390/polym12071558

[34] Al-Itry R., Lamnawar K., Maazouz A.: Improvement of thermal stability, rheological and mechanical properties of PLA, PBAT and their blends by reactive extrusion with functionalized epoxy. Polymer Degradation and Stability, **97**, 1898–1914 (2012). https://doi.org/10.1016/j.polymdegradstab.2012.06.028

[35] Li S., He G., Liao X., Park C. B., Yang Q., Li G.: Introduction of a long-chain branching structure by ultraviolet-induced reactive extrusion to improve cell morphology and processing properties of polylactide foam. RSC Advances, **7**, 6266–6277 (2017). https://doi.org/10.1039/C6RA26457C

[36] Sun Y., Wu L., Bu Z., Li B-G., Li N., Dai J.: Synthesis and thermomechanical and rheological properties of biodegradable long-chain branched poly(butylene succinate-*co*-butylene terephthalate) copolyesters. Industrial and Engineering Chemistry Research, **53**, 10380–10386 (2014). https://doi.org/10.1021/ie501504b

[37] Lu J., Wu L., Li B-G.: Long chain branched poly (butylene succinate-*co*-terephthalate) copolyesters using pentaerythritol as branching agent: Synthesis, thermomechanical, and rheological properties. Journal of Applied Polymer Science, **134**, 44544 (2017). https://doi.org/10.1002/app.44544

[38] Quiles-Carrillo L., Fenollar O., Balart R., Torres-Giner S., Rallini M., Dominici F., Torre L.: A comparative study on the reactive compatibilization of melt-processed polyamide 1010/polylactide blends by multi-function-alized additives derived from linseed oil and petroleum. Express Polymer Letters, **14**, 583–604 (2020). https://doi.org/10.3144/expresspolymlett.2020.48

[39] Cailloux J., Santana O. O., Franco-Urquiza E., Bou J. J., Carrasco F., Gámez-Pérez J., Maspoch M. L.: Sheets of branched poly(lactic acid) obtained by one step reactive extrusion calendering process: Melt rheology analysis. Express Polymer Letters, **7**, 304–318 (2013). https://doi.org/10.3144/expresspolymlett.2013.27

[40] Celli A., Marchese P., Sullalti S., Berti C., Barbiroli G., Commereuc S., Verney V.: Preparation of new biobased polyesters containing glycerol and their photodurability for outdoor applications. Green Chemistry, **14**, 182–187 (2012). https://doi.org/10.1039/C1GC15973A

[41] Härth M., Kaschta J., Schubert D. W.: Shear and elongational flow properties of long-chain branched poly (ethylene terephthalates) and correlations to their molecular structure. Macromolecules, **47**, 4471–4478 (2014). https://doi.org/10.1021/ma5002657

[42] Ren L., Wang Y., Ge J., Lu D., Liu Z.: Enzymatic synthesis of high-molecular-weight poly(butylene succinate) and its copolymers. Macromolecular Chemistry and Physics, **216**, 636–640 (2015). https://doi.org/10.1002/macp.201400550

[43] Wang J-M., Ding S-J., Wu T-M.: Rheology, crystallization behavior, and mechanical properties of poly(butylene succinate-*co*-terephthalate)/cellulose nanocrystal composites. Polymer Testing, **87**, 106551 (2020). https://doi.org/10.1016/j.polymertesting.2020.106551

[44] Garin M., Tighzert L., Vroman I., Marinkovic S., Estrine B.: The influence of molar mass on rheological and di-lute solution properties of poly(butylene succinate). Journal of Applied Polymer Science, **131**, 40887 (2014). https://doi.org/10.1002/app.40887

[45] Härth M., Dörnhöfer A.: Film blowing of linear and long-chain branched poly(ethylene terephthalate). Poly-mers, **12**, 1605 (2020). https://doi.org/10.3390/polym12071605

[46] Charlier Q., Girard E., Freyermouth F., Vandesteene M., Jacquel N., Ladavière C., Rousseau A., Fenouillot F.: Solution viscosity – molar mass relationships for poly (butylene succinate) and discussion on molar mass analysis. Express Polymer Letters, **9**, 424–434 (2015). https://doi.org/10.3144/expresspolymlett.2015.41

[47] Härth M., Dörnhöfer A., Kaschta J., Münstedt H., Schubert D. W.: Molecular structure and rheological properties of a poly(ethylene terephthalate) modified by two different chain extenders. Journal of Applied Polymer Science, **138**, 50110 (2021). https://doi.org/10.1002/app.50110

[48] Nifant'ev I. E., Bagrov V. V., Komarov P. D., Ilyin S. O., Ivchenko P. V.: The use of branching agents in the synthesis of PBAT. Polymers, **14**, 1720 (2022). https://doi.org/10.3390/polym14091720

[49] Standau T., Nofar M., Dörr D., Ruckdäschel H., Altstädt V.: A review on multifunctional epoxy-based Joncryl® ADR chain extended thermoplastics. Polymer Reviews, **62**, 296–350 (2022). https://doi.org/10.1080/15583724.2021.1918710

[50] Jie Z., Fa-xue L., Jiang-yong Y.: Multiple melting behavior of biodegradable poly(butylene succinate-*co*-terephthalate) (PBST) copolyester. Journal of Thermal Analysis and Calorimetry, **111**, 711–715 (2013). https://doi.org/10.1007/s10973-012-2229-2

[51] Li F., Xu X., Hao Q., Li Q., Yu J., Cao A.: Effects of comonomer sequential structure on thermal and crystallization behaviors of biodegradable poly(butylene succinate-*co*-butylene terephthalate)s. Journal of Polymer Science Part B: Polymer Physics, **44**, 1635–1644 (2006). https://doi.org/10.1002/polb.20797

[52] Luo S., Li F., Yu J., Cao A.: Synthesis of poly(butylene succinate-*co*-butylene terephthalate) (PBST) copolyesters with high molecular weights *via* direct esterification and polycondensation. Journal of Applied Polymer Science, **115**, 2203–2211 (2010). https://doi.org/10.1002/app.31346

[53] Luo S., Li F., Yu J.: The thermal, mechanical and viscoelastic properties of poly(butylene succinate-*co*-terephthalate) (PBST) copolyesters with high content of BT units. Journal of Polymer Research, **18**, 393–400 (2011). https://doi.org/10.1007/s10965-010-9429-x

[54] Wojtczak M., Dutkiewicz S., Galeski A., Gutowska A.: Classification of aliphatic-butylene terephthalate copolyesters in relation to aliphatic/aromatic ratio. Polymer, **113**, 119–134 (2017). https://doi.org/10.1016/j.polymer.2017.02.054

[55] Zheng C., Zhu G., Shi Y., Liu L-Z., Ren M., Zhang W., Han L.: Crystallization, structures and properties of biodegradable poly(butylene succinate-*co*-butylene terephthalate) with a symmetric composition. Materials Chemistry and Physics, **260**, 124183 (2021). https://doi.org/10.1016/j.matchemphys.2020.124183

[56] Ishioka R., Kitakuni E., Ichikawa Y.: Aliphatic polyesters: 'Bionolle'. in 'Biopolymers online' (eds.: Hofrichter M., Steinbüchel A.) Wiley-VCH, Weinheim, Vol 4, 275–297 (2002). https://doi.org/10.1002/3527600035.bpol4010

[57] Duborper C., Samuel C., Akue-Asseko A. C., Loux C., Lacrampe M-F., Krawczak P.: Design of biobased poly (butylene succinate) foams by single-screw extrusion: Identification of relevant rheological parameters controlling foam morphologies. Polymer Engineering and Science, **58**, 503–512 (2018). https://doi.org/10.1002/pen.24733

[58] Arayesh H., Ebrahimi N. G., Khaledi B., Esfahani M. K.: Introducing four different branch structures in PET by reactive processing – A rheological investigation. Journal of Applied Polymer Science, **137**, 49243 (2020). https://doi.org/10.1002/app.49243

[59] Han Y-K., Um J. W., Im S. S., Kim B. C.: Synthesis and characterization of high molecular weight branched PBA. Journal of Polymer Science Part A: Polymer Chemistry, **39**, 2143–2150 (2001). https://doi.org/10.1002/pola.1190

[60] Purohit P. J., Huacuja-Sánchez J. E., Wang D-Y., Emmerling F., Thünemann A., Heinrich G., Schönhals A.: Structure–property relationships of nanocomposites based on polypropylene and layered double hydroxides. Macromolecules, **44**, 4342–4354 (2011). https://doi.org/10.1021/ma200323k

[61] Henton D. E., Gruber P., Lunt J., Randall J.: Polylactic acid technology. in 'Natural fibers, biopolymers, and biocomposites' (eds.: Mohanty A. K., Misra L., Drzal L. T.) Taylor and Francis, Michigan, 527–577 (2005). https://doi.org/10.1201/9780203508206

[62] Witzke D. R., Narayan R., Kolstad J. J.: Reversible kinetics and thermodynamics of the homopolymerization of L-lactide with 2-ethylhexanoic acid tin(II) salt. Macromolecules, **30**, 7075–7085 (1997). https://doi.org/10.1021/ma970631m

[63] Gupta M. C., Deshmukh V. G.: Thermal oxidative degradation of poly-lactic acid. Part I: Activation energy of thermal degradation in air. Colloid and Polymer Science, **260**, 308–311 (1982). https://doi.org/10.1007/BF01447969

[64] Sivasamy P., Palaniandavar M., Vijayakumar C., Lederer K.: The role of β-hydrogen in the degradation of polyesters. Polymer Degradation and Stability, **38**, 15–21 (1992). https://doi.org/10.1016/0141-3910(92)90017-Y

[65] Nguyen Q. T., Japon S., Luciani A., Leterrier Y., Månson J-A. E.: Molecular characterization and rheological properties of modified poly(ethylene terephthalate) obtained by reactive extrusion. Polymer Engineering and Science, **41**, 1299–1309 (2001). https://doi.org/10.1002/pen.10830

[66] Yang Z., Xin C., Mughal W., Li X., He Y.: High-melt-elasticity poly(ethylene terephthalate) produced by reactive extrusion with a multi-functional epoxide for foaming. Journal of Applied Polymer Science, **135**, 45805 (2018). https://doi.org/10.1002/app.45805

[67] Dhavalikar R., Yamaguchi M., Xanthos M.: Molecular and structural analysis of a triepoxide-modified poly (ethylene terephthalate) from rheological data. Journal of Polymer Science Part A: Polymer Chemistry, **41**, 958–969 (2003). https://doi.org/10.1002/pola.10641

[68] Chen P., Zhao L., Gao X., Xu Z., Liu Z., Hu D.: Engineering of polybutylene succinate with long-chain branching toward high foamability and degradation. Polymer Degradation and Stability, **194**, 109745 (2021). https://doi.org/10.1016/j.polymdegradstab.2021.109745

[69] Honerkamp J., Weese J.: Determination of the relaxation spectrum by a regularization method. Macromolecules, **22**, 4372–4377 (1989). https://doi.org/10.1021/ma00201a036

[70] Maroufkhani M., Ebrahimi N. G.: Melt rheology of linear and long-chain branched polypropylene blends. Iranian Polymer Journal, **24**, 715–724 (2015). https://doi.org/10.1007/s13726-015-0357-9

[71] Trinkle S., Walter P., Friedrich C.: van Gurp-Palmen plot II – Classification of long chain branched polymers by their topology. Rheologica Acta, **41**, 103–113 (2002). https://doi.org/10.1007/s003970200010

[72] Stadler F. J., Kaschta J., Münstedt H.: Thermorheological behavior of various long-chain branched polyethylenes. Macromolecules, **41**, 1328–1333 (2008). https://doi.org/10.1021/ma702367a

[73] Bourg V., Valette R., le Moigne N., Ienny P., Guillard V., Bergeret A.: Shear and extensional rheology of linear and branched polybutylene succinate blends. Polymers, **13**, 652 (2021). https://doi.org/10.3390/polym13040652

[74] Münstedt H., Kurzbeck S., Stange J.: Importance of elongational properties of polymer melts for film blowing and thermoforming. Polymer Engineering and Science, **46**, 1190–1195 (2006). https://doi.org/10.1002/pen.20588

[75] Liu G., Ma H., Lee H., Xu H., Cheng S., Sun H., Chang T., Quirk R. P., Wang S-Q.: Long-chain branched polymers to prolong homogeneous stretching and to resist melt breakup. Polymer, **54**, 6608–6616 (2013). https://doi.org/10.1016/j.polymer.2013.10.007